Putative Helix F Contributes to Regioselectivity of Hydroxylation in Mitochondrial Cytochrome P450 27A1†

Irina A. Pikuleva,*,‡ Andrei Puchkaev,‡,§ and Ingemar Björkhem||

Department of Pharmacology and Toxicology, University of Texas Medical Branch, Galveston, Texas 77555-1031, and Department of Clinical Chemistry, Karolinska Institute, Huddinge Hospital, S-141 88 Huddinge, Sweden

Received January 30, 2001

ABSTRACT: On the basis of alignment with structurally characterized cytochromes P450 (P450s), we have identified the putative F and G helices of mitochondrial P450s 27A1 and 11A. We introduced substitutions at Phe-207, Ile-211, and Phe-215 within putative helix F and at Trp-235 and Tyr-238 within putative helix G in P450 27A1 and compared wild type and mutants with respect to catalytic activity, product pattern, substrate binding, formation of hydrogen peroxide, and interaction with redox partner. Results indicate that the mutated residues are important for delivery of the correctly oriented substrate to the P450 active site. The I211K and F215K mutations, for example, affected the regioselectivity of P450 27A1-dependent hydroxylation reactions and conferred the P450 capacity to cleave the C−C bond of the substrate during the catalytic cycle. Studies of P450 11A1 indicate that Phe-202 has functions similar to those of its counterpart in P450 27A1 (Phe-215). We propose that putative helices F and G form the sides of the substrate-access channel, thus providing the additional mechanism to control regioselectivity of hydroxylation in mitochondrial P450s.

Mitochondrial cytochromes P450 (P450s) play important physiological roles in mammals due to their involvement in bile acid and steroid hormone biosynthesis and in the metabolism of vitamin D_3. The present study focuses on two mitochondrial P450s, 27A1 and 11A1. The ubiquitously expressed P450 27A1 catalyzes multiple oxidation reactions at the C27 atom of bile acid intermediates in liver and cholesterol in extrahepatic tissues (*1*, *2*). P450 11A1 is expressed primarily in steroidogenic tissues, where it converts cholesterol to pregnenolone, the first and rate-limiting step in steroid hormone biosynthesis (*3*). P450s 27A1 and 11A1 have been cloned (*4*, *5*) and overexpressed in *Escherichia coli* (*6*, *7*); however, little is known about how these P450s interact with the physiological substrates.

To begin to elucidate the molecular basis for substrate specificity and regioselectivity of hydroxylation reactions in mitochondrial P450s, we capitalized on the knowledge derived from determination and comparison of the crystal structures of seven different P450s which belong to distinct gene families (101, 108, 102, 107A1, 55A1, 2C5, and 119) (*8*−*14*). All structurally characterized P450s have a similar overall fold and contain a number of conserved topological elements (*15*). Interaction with substrate in these P450s is realized through a limited number of amino acid residues, many of which are located at the same (or very close to) alignment positions (*16*). These residues hold the substrate in an orientation that allows regio- and stereoselective hydroxylation. Unlike many enzymes, the active site of structurally characterized P450s does not form an open cleft at the molecular surface but is buried inside the molecule. A well-defined channel (substrate-access channel) connecting the protein surface and the substrate-binding site is seen in the structure of only one P450, 102 (*9*), and it is postulated that substrate entry in P450s is controlled by the opening motion of the substrate-access channel. It remains to be elucidated whether the same topological elements form sides of the substrate-access channel in all P450s and whether the substrate-access channel is preserved in membrane-bound P450s, in which lipophilic substrates enter the enzyme directly from the lipid bilayer. Peterson and colleagues have suggested that residues lining the interior of the substrate-access channel could also contribute to substrate specificity and influence the P450 product pattern because such residues may determine the orientation of the substrate as it enters the P450 active site (*17*).

Structural studies have identified helices F and G as topological elements that are being conserved in the P450 superfamily, although their spatial disposition relative to heme, size, and role varies among structurally characterized P450s. In P450 102, helices F and G form both sides of the substrate-access channel and the ceiling of the active site (*9*). In P450 101, they define the top of the active site (*8*), while in P450s 107A1 and 2C5, only helix F forms the ceiling of the active site (*11*, *13*). High spatial variability precludes reliable prediction of the role of these topological elements in P450s with unknown structures. Herein we describe the effect of mutation of amino acid residues located within the putative helices F and G in human P450 27A1 and bovine P450 11A1 and discuss their possible role in the

† These studies were supported in part by the John Sealy Memorial Endowment Fund (to I.A.P.), Center Grants ES00267 and ES06676, grants from the Swedish Medical Research Council and Heart-Lung Foundation (to I.B.), and U.S. Public Health Service Grant GM37942.

* To whom correspondence should be addressed. Telephone: (409) 772-9657. Fax: (409) 772-9642. E-mail: irpikule@utmb.edu.

‡ University of Texas Medical Branch.

§ Permanent address: Institute of Bioorganic Chemistry, Byelorussian Academy of Sciences, Minsk 220141, Belarus.

|| Karolinska Institute.

10.1021/bi010193i CCC: $20.00
Published on Web 05/26/2001

Table 1: Oligonucleotides and Templates Used To Generate P450s 27A1 and 11A1 Mutants

template	mutation	oligonucleotides
P450 27A1	F207K	5′-GGACACCGTGACCAAGGTCAGATCCATCG-3′ [a] 5′-CGATGGATCTGACCTTGGTCACGGTGTCC-3′
P450 27A1	I211K	5′-CCTTCGTCAGATCTAAGGGGTTAATGTTCC-3′ 5′-GGAACATTAACCCCTTAGATCTGACGAAGG-3′
P450 27A1	F215K	5′-CCATCGGGTTAATGAAACAGAACTCACTC-3′ 5′-GAGTGAGTTCTGTTTCATTAACCCGATGG-3′
P450 27A1	F215A	5′-ATCGGGTTAATGGCCCAGAACTCACTCTATGCC-3′ 5′-GGCATAGAGTGAGTTCTGGGCCATTAACCCGAT-3′
F215K P450 27A1	I211K/F215K	5′-CCTTCGTCAGATCTAAGGGGTTAATGAAAC-3′ 5′-GTTTCATTAACCCCTTAGATCTGACGAAGG-3′
I211K/F215K P450 27A1	F207K/I211K/F215K	5′-GACACCGTGACCAAGGTCAGATCTAAGGGG-3′ 5′-CCCCTTAGATCTGACCTTGGTCACGGTGTC-3′
F215A P450 27A1	F207A/I211A/F215A	5′-GACACCGTGACCGCGGTCAGATCCGCCGGCTTAATGGCCC-3′ 5′-GGGCCATTAAGCCGGCGGATCTGACCGCGGTCACGGTGTC-3′
P450 27A1	W235A	5′-CCCGTGCTGCCTTTCGCGAAGCGATACCTGGATGGT-3′ 5′-ACCATCCAGGTATCGCTTCGCGAAAGGCAGCACGGG-3′
P450 27A1	Y238A	5′-CCTTTCTGGAAGCGAGCGCTGGATGGTTGGAATGCC-3′ 5′-GGCATTCCAACCATCCAGCGCTCGCTTCCAGAAAGG-3′
P450 11A1	F202A	5′-GCCGTCTACAAGATGGCCCACACCAGTGTCCCT-3′ 5′-AGGGACACTGGTGTGGGCCATCTTGTAGACGGC-3′
P450 11A1	F202K	5′-GCCGTCTACAAGATGAAACACACCAGTGTCCCT-3′ 5′-AGGGACACTGGTGTGTTTCATCTTGTAGACGGC-3′

[a] The mutated nucleotides are underlined.

mechanism of regioselectivity of hydroxylation in mitochondrial P450s.

EXPERIMENTAL PROCEDURES

Site-Directed Mutagenesis. This was carried out using an in vitro QuikChange site-directed mutagenesis kit (Stratagene) according to the instructions. The templates and complementary mutagenic oligonucleotides are shown in Table 1. Mutations were confirmed by DNA sequencing. The *Kpn*I/*Stu*I fragments of human P450 27A1 and *Bam*HI/*Bgl*II fragments of bovine P450 11A1 containing the mutations were ligated into *Kpn*I/*Stu*I- and *Bam*HI/*Bgl*II-digested expression constructs containing wild-type P450 27A1 and P450 11A1, respectively. For each mutant the region upstream of the *Kpn*I site to beyond the *Stu*I site (P450 27A1) or from *Bam*HI to *Bgl*II sites (P450 11A1) was sequenced to ensure there were no undesired mutations and to confirm correct ligation.

Subcellular Fractionation of the Mutant P450s in E. coli. E. coli cultures were grown and harvested as described previously (*7*, *18*). Spheroplasts were prepared by suspending cells in 10% of the original culture volume in 10 mM potassium phosphate buffer (KP_i), pH 7.4, containing 20% glycerol. The cell suspension was incubated with lysozyme (0.5 mg/mL) for 30 min at 4 °C. Spheroplasts were pelleted at 5000*g* for 10 min and then resuspended in 10 mM KP_i, pH 7.4, containing 20% glycerol, 0.5 mM phenylmethanesulfonyl fluoride, 0.5 μg/mL leupeptin, 2 μg/mL aprotinin, and 1 μg/mL pepstatin. After sonication on ice using six 20 s pulses at 1 min intervals, cell debris was removed at 5000*g* (10 min). The supernatant and pellet obtained after subsequent ultracentrifugation at 106000*g* for 60 min were used as cytosolic and membrane fractions, respectively.

Purification of Mutant P450s. The purification procedure for both P450 27A1 and P450 11A1 wild types or mutants was as that described for P450 27A1 (*7*). Wild-type and mutant forms were concentrated and dialyzed overnight against 100 volumes of 40 mM KP_i, pH 7.4, containing 20% glycerol, and frozen at −80 °C.

Enzyme Assays. Enzymatic activities of wild-type and mutated forms of P450 27A1 and P450 11A1 were determined as described (*7*, *18*). To determine the turnover number of the P450 27A1 mutants toward 5β-cholestane-3α,7α,12α-triol, the reaction conditions were optimized for the formation of one product only, 5β-cholestane-3α,7α,12α,27-tetrol, linear with time and protein. Reconstituted P450 27A1 systems (wild type or mutant) contained varying amounts of P450 (0.014−0.3 μM), 1.0 μM adrenodoxin reductase (Adr), 5.0 μM adrenodoxin (Adx), 50 μM 5β-cholestane-3α,7α,12α-triol, 5β-[^{3}H]cholestane-3α,7α,12α-triol (250 000 cpm), 1 mM NADPH, and 40 mM KP_i, pH 7.4. The reaction time was 5−10 min. The wild-type and mutant P450s 11A1 were assayed using 0.1−2.0 μM P450, 1.0−2.0 μM Adr, 5.0−10.0 μM Adx, 50 μM cholesterol, [^{3}H]cholesterol (250 000 cpm), 1 mM NADPH, and 40 mM KP_i, pH 7.4, and the reaction time was 1−15 min. The following modifications, which did not affect the turnover numbers, were introduced in the P450 11A1 enzyme assay: Tween 20 was omitted, and a stock solution of cholesterol (10 mM) was prepared using a 45% aqueous solution of 2-hydroxypropyl-β-cyclodextrin. This was done because studies of cholesterol binding (described below) were carried out in the absence of Tween 20 using a stock solution of cholesterol in 2-hydroxypropyl-β-cyclodextrin.

Identification of Unknown Metabolites. Reaction conditions have been optimized for maximal product formation: the reaction time was 1−2 h, and concentrations of mutant P450s 27A1 and 11A1, Adx, and Adr varied from 1 to 4 μM, 5−20 μM, and 1−4 μM, respectively. Products were extracted with CH_2Cl_2, evaporated, and separated by HPLC. Individual fractions were then analyzed as trimethylsilyl ethers or methyl ester trimethylsilyl ethers by combined gas chromatography−mass spectrometry (GC−MS) (*19*).

Interaction with Adx. This was monitored using affinity chromatography on Adx−Sepharose as described (*20*).

Substrate Binding Assays. Apparent binding constants (K_d) of P450 27A1 wild type or mutants for 5β-cholestane-3α,7α,12α-triol and P450 11A1 wild type or mutants for

cholesterol were determined as described (*18*). P450 27A1 wild type and mutants (0.3 μM) were titrated with 5β-cholestane-3α,7α,12α-triol dissolved in ethanol. The buffer (50 mM KP_i, pH 7.4) also contained 20% glycerol. In our preliminary studies we established that 20% glycerol did not affect the K_d for 5β-cholestane-3α,7α,12α-triol, whereas 0.1% Tween 20, often used to improve solubility of hydrophobic substrates, increased the K_d 70-fold. Titrations of P450 11A1 wild type (0.3 μM) and the F202A and F202K mutants (0.3 and 2.4 μM, respectively) were also carried out in 50 mM KP_i detergent-free buffer. Highly hydrophobic cholesterol was added from a stock solution in 45% 2-hydroxypropyl-β-cyclodextrin because cyclodextrin-solubilized compounds do not precipitate upon dilution in aqueous solutions (*21*). Under these conditions, the apparent K_d for cholesterol was 17 times less than that determined in the presence of 0.1% Tween 20 using ethanol-dissolved cholesterol (*18*). To completely eliminate partial denaturation of the F202A P450 11A1 mutant that was observed at 18 °C or in the presence of 20% glycerol, all titrations of the P450 11A1 enzymes were carried out at 12 °C. In a separate experiment, we established that a decrease in temperature by 6 °C does not alter the K_d of the wild-type P450 11A1 for cholesterol. In all experiments P450 content was quantified by a reduced CO difference spectrum (*22*) to confirm that there was no enzyme denaturation during titration.

Measurement of Hydrogen Peroxide Production. This was carried out in reconstituted systems containing 0.3 μM P450 27A1 wild type or mutants, 1 μM Adr, 4 μM Adx, 50 μM 5β-cholestane-3α,7α,12α-triol, 5β-[^{3}H]cholestane-3α,7α,12α-triol (250 000 cpm), 1 mM NADPH, and 40 mM KP_i, pH 7.4 (P450 27A1-dependent enzymatic assay), and 2 μM P450 11A1 wild type or mutants, 2 μM Adr, 10 μM Adx, 50 μM cholesterol, [^{3}H]cholesterol (250 000 cpm), 1 mM NADPH, and 40 mM KP_i, pH 7.4 (P450 11A1-dependent enzymatic assay). The H_2O_2 was determined using xylenol orange colorimetric assay (*23*, *24*). Measurements with this assay require iron-free solutions and were accomplished by passing phosphate buffer and deionized, doubly distilled water used for solution preparation through a Chelex column. All glassware was rinsed with iron-free water. Immediately after addition of NADPH (zero time) and after 10 min of the NADPH-initiated enzymatic reaction, 100 μL (1/10) of the reaction mixture was added to 890 μL of 25 mM H_2SO_4 containing 120 mM sorbitol which quenches the enzymatic reaction. Brief vortexing was followed by addition of 17.5 μL of the color-developing agent (1 volume of 20 mM xylenol orange mixed with 2.5 volumes of 20 mM fresh ferrous ammonium sulfate) and incubation at room temperature for 45 min. After removal of precipitated proteins (13000*g*, 5 min), absorbance (560 nm) of the solution quenched at 10 min was read against that of the solution quenched at zero time. The H_2O_2 concentration was determined from a calibration curve using a series of H_2O_2 dilutions from a 30% stock solution. The exact concentration of H_2O_2 in the stock solution was determined spectrophotometrically using the extinction coefficient of 43.6 M^{-1} cm^{-1} at 240 nm (*22*). Solutions for the calibration curve contained 100 μL of the reaction mixture quenched at zero time with 890 μL of 25 mM H_2SO_4 containing 120 mM sorbitol, 10 μL of H_2O_2 of different dilutions, and 17.5 μL of the color-developing agent. Absorbance was read at 560 nm against the reference solution containing no H_2O_2.

Parallel to measurement of hydrogen peroxide production, the formation of the P450 27A1 and P450 11A1 products was quantified (*25*) by extracting steroids with CH_2Cl_2 immediately after the second aliquot of the reaction mixture (100 μL) was taken for H_2O_2 determination.

RESULTS

Mutagenesis Strategy. Phe-215 in P450 27A1 was mutated because it aligns with Leu-175 in P450 107A1, Leu-208 in P450 2C5, and Thr-185 in P450 101, residues that interact with substrate in these structurally characterized P450s (Figure 1), and is conserved among mitochondrial P450s that metabolize substrates derived from cholesterol (P450s 27A1, 11A1, 11B1, 11B2, and 11B3, Figure 1). After the properties of the F215A and F215K mutants were determined, two additional single mutants (F207K and I211K) and, later, one double (I211K/F215K) and two triple (F207A/I211A/F215A and F207K/I211K/F215K) mutants were generated. Phe-207 and Ile-211 were selected because they are located on the same side of the putative F helix, three and seven residues away from Phe-215. Phe-207 is also conserved in all mammalian mitochondrial P450s, implying that it may play a specific role in this subset of P450s. Ile-211 was selected because this alignment position is always occupied by an aliphatic amino acid residue in mitochondrial P450s (Figure 1). To probe the role of the N-terminal part of the putative helix G in P450 27A1, two hydrophobic residues Trp-235 and Tyr-238, supposedly located on the opposite sides of the helix, were mutated to alanine. One of these residues, Trp-235, is conserved among mitochondrial P450s (Figure 1). To compare the effect of mutation between two mitochondrial P450s, Phe-202, a residue aligning with Phe-215 in P450 27A1, was mutated in P450 11A1 (Figure 1).

Expression and Subcellular Distribution of the P450 27A1 Mutants. All of the mutants except one (F207K/I211K/F215K) were overexpressed at levels comparable with that of the wild-type enzyme. The F207K/I211K/F215K *E. coli* lysate showed no detectable protein on a Western blot, indicating that proper folding of this mutant is most probably disrupted and it is digested by proteases.

The region between helices F and G, the F−G loop, is proposed to contribute to membrane binding in microsomal P450s (*17*). However, in P450 2C5, the site of attachment to membrane comprises not only the F−G loop but the F helix as well (*26*). By using Western blot analysis we investigated the effect of single mutations within putative helices F and G on the subcellular localization of P450 27A1. None of the single mutations within the putative helix F in P450 27A1 (F207K, I211K, or F215K) resulted in a cytosolic protein; however, a small portion of the W235A mutant and trace amounts of the Y238A mutant (putative helix G) were detected in the cytosol in low ionic strength buffer (Figure 2). This is concordant with our most recent studies (not shown) indicating that a region comprising residues 230−237 (the C-terminal part of the F−G loop and the N-terminus of the G helix) contributes to membrane association in P450 27A1. The fact that the W235A mutation affected the subcellular distribution of the protein also suggests that Trp-235 is located on the surface of the molecule in P450 27A1.

Catalytic Activity of the P450 27A1 Mutants. P450 27A1 is capable of oxidizing the C27 atom of 5β-cholestane-

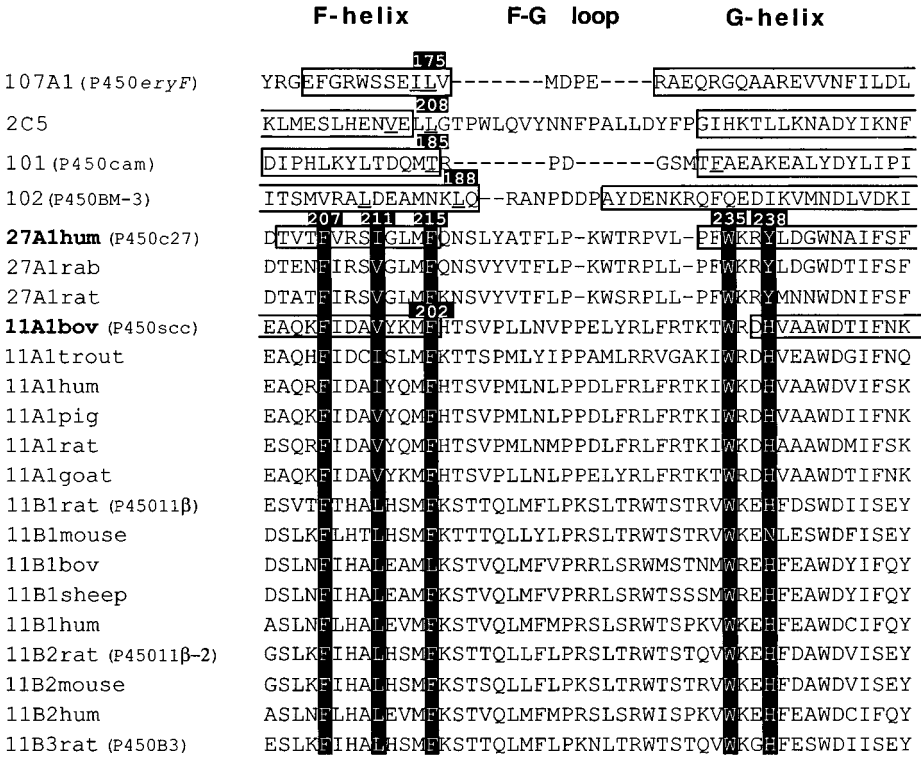

FIGURE 1: Alignment of amino acid sequences of mitochondrial P450s and structurally characterized P450s 107A1, 101, and 102 in the region of the putative F and G helices and the F−G loop. The trivial names of the P450s are shown in parentheses. Original references for these sequences can be found in the P450 superfamily summary (*39*). Boxes indicate α-helices. Secondary structural elements of P450 27A1 and 11A1 are predicted using the self-optimized prediction method (the web site is http://pbil.ibcp.fr). Structural alignments of P450s 107A1 and 101 and of 101 and 102 are taken from refs *11* and *9*, respectively. Residues mutated in P450s 27A1 and 11A1 are boxed in black.

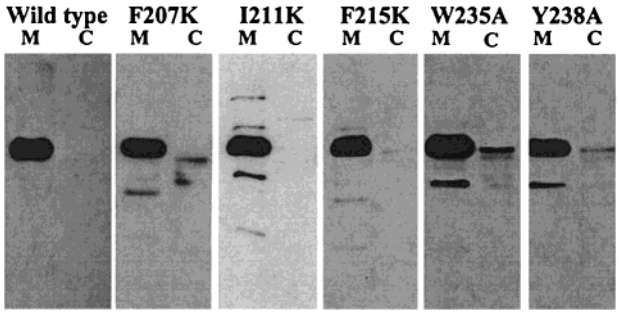

FIGURE 2: Subcellular distribution of the P450 27A1 mutants in low ionic strength buffer (10 mM KP_i, pH 7.4, 20% glycerol). The samples (5 μg of total protein) were analyzed by Westerm blotting using antibodies against P450 27A1. M and C indicate the membrane fraction and cytosol, respectively.

3α,7α,12α-triol three times to give at first 5β-cholestane-3α,7α,12α,27-tetrol, then 3α,7α,12α-trihydroxy-5β-cholestan-27-al, and finally 3α,7α,12α-trihydroxy-5β-cholestanoic acid (*27*) (Figure 3). P450 27A1 was also shown to perform 24- and 25-hydroxylation (*28*), although the rate of these hydroxylations was markedly lower than the corresponding rate of 27-hydroxylation of the same substrate. A significant isotope effect was observed in the case of 24-hydroxylation, but not with 25- or 27-hydroxylation, indicating that the mechanism of interaction between the substrate and the enzyme differs for 24-hydroxylation (*28*). Catalytic activities of P450 27A1 wild type and mutants were assayed under the conditions when only a single metabolite, 5β-cholestane-3α,7α,12α,27-tetrol, was formed from 5β-cholestane-3α,7α,12α-triol. As is seen from Table 2, enzymatic activity of all mutants was decreased compared to that of the wild type. All single alanine mutants of P450 27A1 (F215A, W235A, and Y238A) exhibited only a moderate decrease in enzymatic activity (30−45%), while single substitutions with lysine (F207K, I211K, and F215K) resulted in a 10−25-fold reduction of the turnover number. The activity of a double lysine mutant (I2111K/F215K) was comparable to that of single mutants, indicating the lack of additivity for the I211K and F215K mutations. A triple alanine F207A/I2111A/F215A mutation also led to a significant reduction in the turnover number (12% of the wild-type activity). Thus, there seems to be a correlation between the hydrophobicity of the side chain at positions 207, 211, and 215 and P450 27A1 enzymatic activity: more polar amino acid substitutions cause a more pronounced decrease in enzymatic activity.

Metabolites of the P450 27A1 Mutants. We also investigated the effect of mutations on the P450 27A1 product pattern. As assessed by GC−MS, 3α,7α,12α-trihydroxy-5β-cholestanoic acid and small amounts of 3α,7α,12α-trihydroxy-5β-cholestan-27-al were the only products when 90% of 5β-cholestane-3α,7α,12α-triol was metabolized by the F207K, F215A, F207A/I211A/F215A, W235A, and Y238A P450 27A1 mutants. Only traces of other metabolites were present in these incubations. In contrast, incubations of the I211K, F215K, and I211K/F215K mutants with 5β-cholestane-3α,7α,12α-triol contained much higher amounts of the non-C27-oxidized steroids. The formation of these products was found to be time (Figure 4) and P450 (not shown) dependent. To identify these products, extract after the reaction of the F215K mutant with 5β-cholestane-3α,7α,12α-

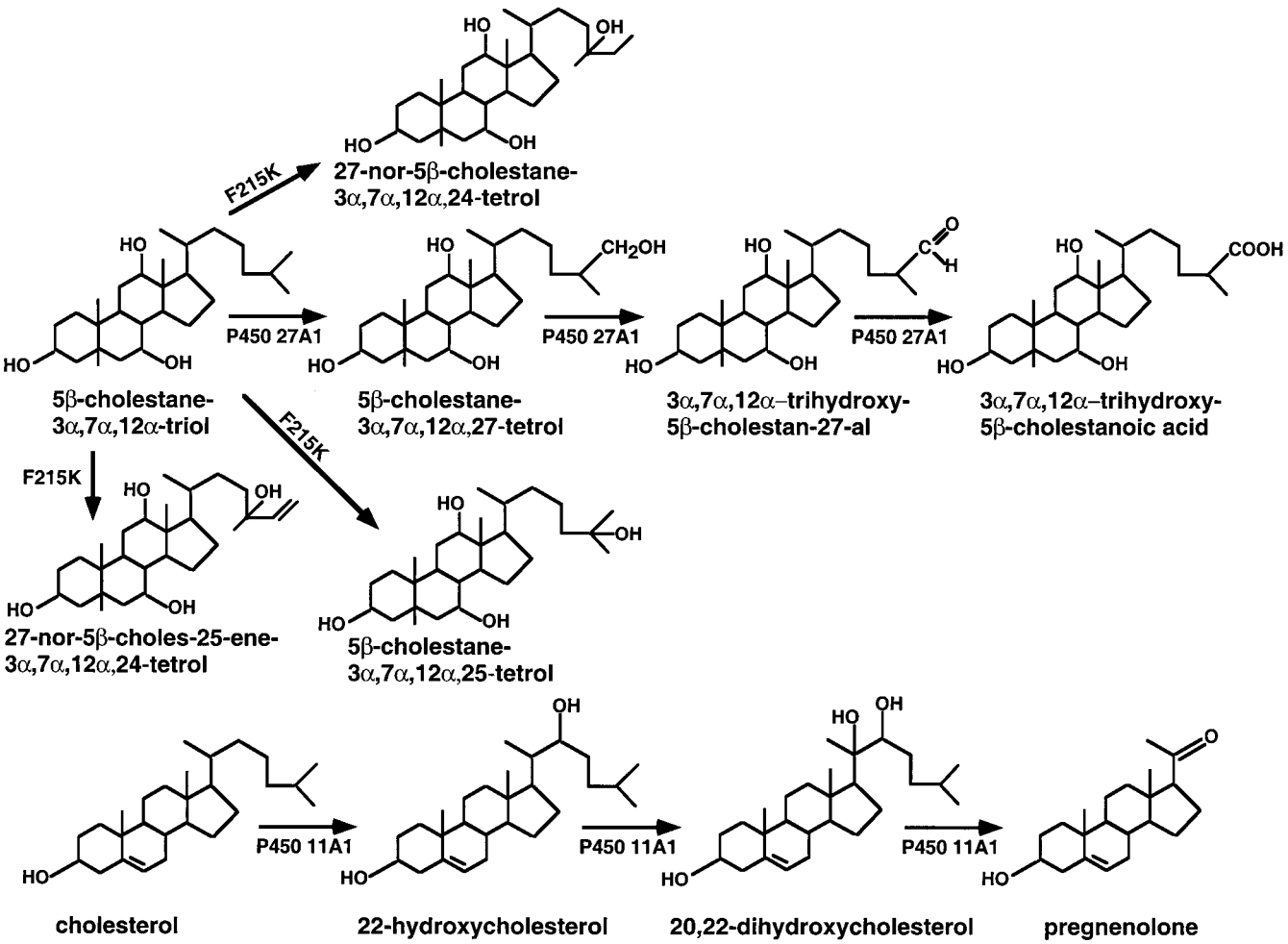

FIGURE 3: Products found in the incubations of P450 27A1 wild type and the F215K mutant with 5*β*-cholestane-3α,7α,12α-triol and P450 11A1 with cholesterol.

triol was separated by HPLC (Figure 4C), and individual fractions were analyzed by GC−MS. Peaks 1 contained 5*β*-cholestane-3α,7α,12α-triol, and peaks 2 and 3 (Figure 4C) were mainly the usual products of 27-hydroxylase activity, 5*β*-cholestane-3α,7α,12α,27-tetrol and 3α,7α,12α-trihydroxy-5*β*-cholestanoic acid, respectively. In the combined pool of products eluting between peaks 2 and 3 in Figure 4C, the trimethylsilyl ether of the most prominent of the unusual metabolites gave a mass spectrum (Figure 5A) that corresponded to a demethylated tetrahydroxylated bile alcohol (a C26 steroid) with a hydroxyl group or a double bond in the steroid side chain. Characteristic peaks were seen at *m*/*z* 620 (M − 90), *m*/*z* 530 (M − 2 × 90), *m*/*z* 440 (M − 3 × 90), and *m*/*z* 343 (loss of the steroid side chain and all trimethylsilyl groups). In the above interpretations, it is assumed that a hydroxyl group is present in the steroid side chain.

Another less prominent metabolite gave a similar mass spectrum (Figure 5B), but in addition fragments were seen at *m*/*z* 501 and *m*/*z* 411, corresponding to the loss of the two terminal carbon atoms of the steroid side chain from the ions with *m*/*z* 530 and *m*/*z* 440, respectively. Also, there was a prominent peak at *m*/*z* 131, corresponding to one trimethylsilyl group and three carbon atoms from the steroid side chain (not seen in the figure). The latter fragmentation suggests that the compound is identical to 27-nor-5*β*-cholestane-3α,7α,12α,24-tetrol (Figure 3). A mass spectrum of this compound was reported previously (*29*).

One additional metabolite had a mass spectrum showing peaks at *m*/*z* 618, *m*/*z* 528, *m*/*z* 438, *m*/*z* 343, *m*/*z* 281, and *m*/*z* 253 (Figure 5C), corresponding to a C26 bile alcohol with two hydroxyl groups or one hydroxyl group and one double bond in the steroid side chain. An almost identical mass spectrum has been published for 27-nor-5*β*-cholest-25-ene-3α,7α,12α, 24-tetrol (Figure 3) (*30*). Finally, trace amounts of 5*β*-cholestane-3α,7α,12α,25-tetrol (Figure 3) were observed, as shown from the characteristic base peak at *m*/*z* 131 in the mass spectrum of the trimethylsilyl derivative and ions at *m*/*z* 544 (M − 90), 454 *m*/*z* (M − 2 × 90), *m*/*z* 343, and *m*/*z* 253 (*31*).

To the best of our knowledge, this is the first report that mutation conferred the P450 capacity to cleave the C−C bond. We are aware of only one mammalian P450 (CYP51) that possesses demethylase activity and four mammalian P450s (11A1, 17, 19, and 24) that cleave the C−C bond of the substrate during the catalytic cycle. Unfortunately, the specific features that allow these P450s to cleave the C−C bond are not yet known, and the appearance of the rare demethylase activity does not help us to further clarify the role of Ile-211 and Phe-215 in P450 27A1. The C26 bile alcohols produced as a result of demethylase activity of the Ile-211 and F215K mutants are found in small quantities in human bile (*29*) and in large quantities in the bile of lower vertebrates (*28*), yet their metabolic origin has not been

Table 2: Enzymatic Activities and Spectral Binding Properties of P450s 27A1 and 11A1 Wild Type and Mutants

form	turnover,[a] min^{-1}	K_d,[b] μM	ΔA_{max}[b]
wild-type P450 27A1	52.8 ± 4.8	0.69 ± 0.13	0.025 ± 0.001
F207K	4.3 ± 0.2★	0.57 ± 0.11	0.028 ± 0.004
I211K	5.5 ± 0.4★	0.49 ± 0.06	0.017 ± 0.002★
F215K	2.3 ± 0.1★	0.98 ± 0.09★	0.011 ± 0.001★
F215A	31.8 ± 3.2★	0.91 ± 0.04★	0.025 ± 0.001
I211K/F215K	3.0 ± 0.2★	0.41 ± 0.04★	0.016 ± 0.001★
F207A/I211A/F215A	6.5 ± 0.1★	0.36 ± 0.03★	0.020 ± 0.001
W235A	36.9 ± 0.2★	0.39 ± 0.05★	0.022 ± 0.002
Y238A	30.0 ± 0.1★	0.72 ± 0.04	0.041 ± 0.001★
wild-type P450 11A1	13.8 ± 1.7	0.30 ± 0.03	0.064 ± 0.003
F202A	0.03 ± 0.01★	0.37 ± 0.05[c]	*0.022 ± 0.003*[c] ★ (0.003 ± 0.0004)
F202K	1.8 ± 0.2★	0.04 ± 0.01★	0.011 ± 0.001★

[a] Enzymatic activities were measured as described under Experimental Procedures using 5β-cholestane-3α,7α,12α-triol and cholesterol as substrates for P450s 27A1 and 11A1, respectively. The results are the mean ± standard deviation of three to four experiments. Mean values that are significantly different ($p < 0.05$) from those of wild-type P450s 27A1 and 11A1 are designated by a star. [b] Calculated on the basis of spectral binding assays as described under Experimental Procedures using 0.3 μM P450 and 5β-cholestane-3α,7α,12α-triol and cholesterol as substrates for P450s 27A1 and 11A1, respectively. The results are the mean ± standard deviation of three to four experiments. Mean values that are significantly different ($p < 0.05$) from those of wild-type P450s 27A1 and 11A1 are designated by a star. [c] The concentration of this mutant was increased 8-fold (2.4 μM) to detect low/high spin shift. The number in parentheses shows ΔA_{max} normalized to the 0.3 μM P450 concentration.

established. Because some of the products obtained by the F215K mutant are present in bile, the question is raised as to whether P450 27A1 is, in fact, responsible for the natural formation of these products. Since great quantities of steroids are processed by P450 27A1 each day (about 500 mg), even a very tiny formation of side products may be detectable if their biological half-life is sufficiently long. Thus, GC−MS analysis clearly demonstrated that the putative helix F contributes to the regioselectivity of hydroxylation reactions in P450 27A1, and by introduction of a positive charge at positions 211 and 215, it is possible to enhance the minor activities and produce a novel demethylase activity, presumably because of alteration of the substrate orientation in the enzyme active site.

Catalytic Activity and Metabolites of the P450 11A1 Mutants. Both F202K and F202A P450 11A1 mutants had very low enzymatic activity (Table 2), and both mutations led to the appearance of two additional peaks (2 and 3) in HPLC product profiles (Figure 6). The formation of pregnenolone from cholesterol by P450 11A1 requires three hydroxylation steps and proceeds via two hydroxycholesterol intermediates, 22*R*-hydroxycholesterol and 20α,22*R*-dihydroxycholesterol (Figure 3), which are not released from the enzyme active site during the catalytic cycle (*32*). The disappearance of peaks 2 and 3 in the HPLC product profile of the F202K mutant and peak 2 of the F202A mutant (Figure 6), following increases in P450 concentrations and reaction time, greatly suggests that these peaks are the intermediate hydroxycholesterols. We isolated peak 3 of the F202A mutant that was observed under various conditions of enzyme assay (Figure 6). Combined GC−MS gave a mass spectrum of a monotrimethylsilyl ether derivative of the material that was identical to that of the same derivative of 20α,22*R*-dihydroxycholesterol. Intensive peaks were seen at *m*/*z* 173 (fragment corresponding to C22 − C27 + OTmSi), *m*/*z* 281 (M − 173 − 90 − 18), *m*/*z* 299 (M − 173 − 90), *m*/*z* 371 (M − 173 − 18), and *m*/*z* 389 (M − 173) (*33*). One of the hydroxyl groups in the steroid side chain (at C20) is sterically hindered and is not derivatized under the conditions employed. Thus, one of the reasons for the significantly decreased activity of the F202A and F202K mutants is release of the intermediate hydroxycholesterols from the enzyme active site.

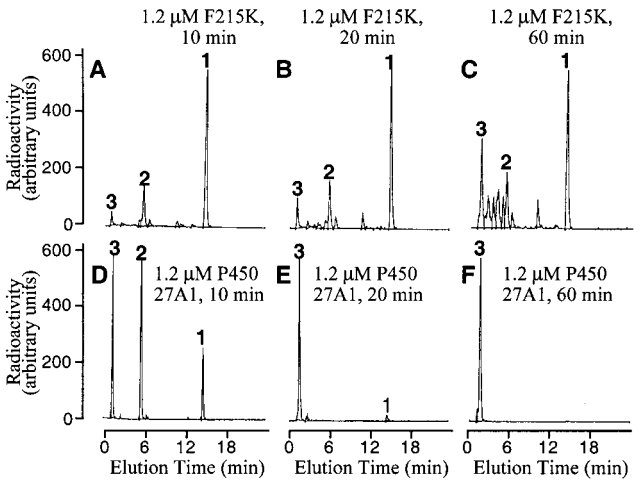

FIGURE 4: Time course of the product formation (as assessed by HPLC separation) in incubations of the 1.2 μM F215K P450 27A1 mutant (A−C) and 1.2 μM wild-type enzyme (D−F) with 50 μM 5β-cholestane-3α,7α,12α-triol: 1, 5β-cholestane-3α,7α,12α-triol; 2, 5β-cholestane-3α,7α,12α,27-tetrol; 3, 3α,7α,12α-trihydroxy-5β-cholestanoic acid. HPLC was performed using a Waters HPLC (Waters Corp., Milford, MA) equipped with a Nova-Pak C_{18} column (3.9 × 150 mm) and a precolumn of the same type connected to a β-RAM radioactivity flow detector (INUS Systems Inc., Tampa, FL). A linear solvent gradient between solvent A (acetonitrile:methanol:water, 40:40:20) and solvent B (100% methanol) over 25 min was used. The flow rate was 1.5 mL/min. Data were analyzed using the Millenium software (Waters Corp., Milford, MA).

Spectral Assays of Substrate Binding. Apparent dissociation constants and maximal amplitudes of substrate-induced spectral responses (ΔA_{max}) of wild-type and mutant P450s are summarized in Table 2. On the basis of substrate-binding properties, the mutants could be arbitrarily placed into four groups. The first group includes the F207K, F207A/I211A/F215A, F215A, and W235A P450 27A1 mutants, which have either unchanged or slightly changed K_d (up to 1.9-fold) and unchanged ΔA_{max}, indicating that residues at positions 207, 211, 215, and 235 in P450 27A1 are not directly involved in binding 5β-cholestane-3α,7α,12α-triol.

The second group is represented by the I211K, I211K/F215K, and F215K P450 27A1 mutants and the F202A P450 11A1 mutant. The K_d of these mutants was also either unchanged or changed only slightly (up to 1.7-fold); however, the ΔA_{max} was decreased 1.5−2.3-fold in the case of the P450 27A1 mutants and more than 20-fold for the F202A P450 11A1 mutant. To detect the spectral response of the F202A P450 11A1 mutant, enzyme concentration was increased 8-fold. If the extinction coefficient of P450 is not affected by mutation, the ΔA_{max} reflects the amount of the enzyme−substrate complex formed. All purified P450 27A1 and 11A1 mutants exhibited UV and visible spectra indistinguishable from the those of wild-type P450s. They all were

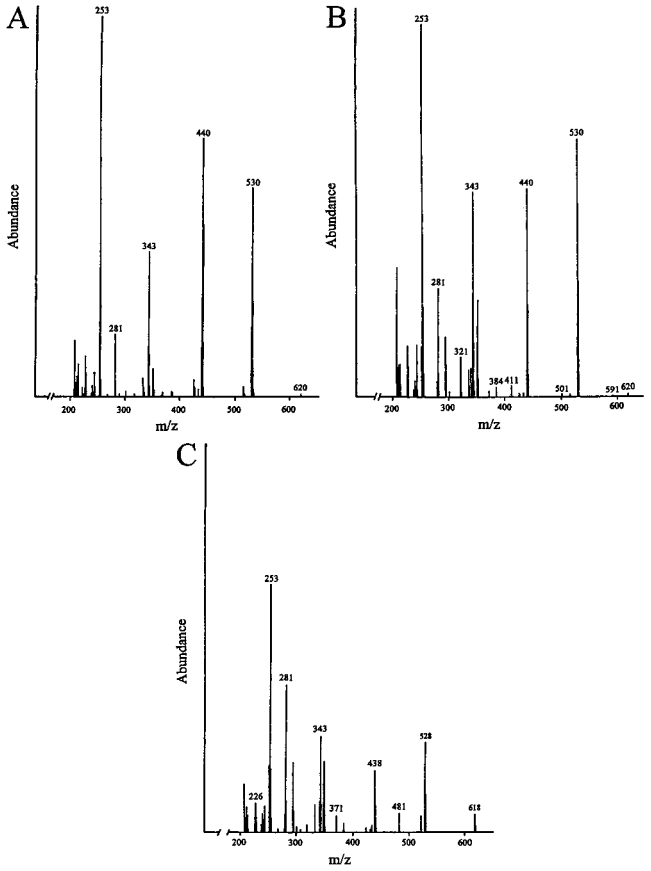

FIGURE 5: Mass spectra of trimethylsilyl ethers of the unusual P450 27A1 metabolites eluting between peaks 2 and 3 in Figure 4C. Panel A corresponds to a demethylated tetrahydroxylated bile alcohol (a C26 steroid) with a hydroxyl group or a double bond in the steroid side chain; panel B corresponds to 27-nor-5β-cholestane-3α,7α,-12α,24-tetrol; panel C corresponds to 27-nor-5β-cholest-25-ene-3α,7α,12α, 24-tetrol.

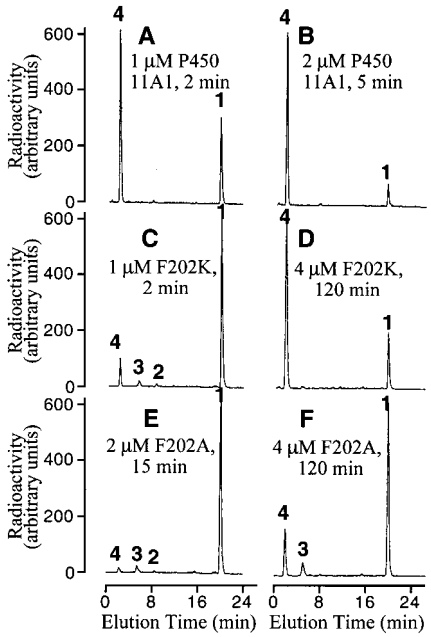

FIGURE 6: Product formation (as assessed by HPLC separation) in incubations of the P450 11A1 wild type (A and B) and F202K (C and D) and F202A (E and F) mutants with cholesterol: 1, cholesterol; 2, 22*R*-hydroxycholesterol; 3, 20α,22*R*-dihydroxycholesterol; 4, pregnenolone. HPLC separation was performed as described in Figure 4, except a linear solvent gradient between solvent A (acetonitrile:methanol:water, 40:40:20) and solvent B (100% methanol) over 15 min was used, after which the flow was kept at 100% solvent B for another 10 min.

isolated as substrate-free, low-spin forms with specific heme contents of 17−17.5 nmol/mg of protein. The same amounts of wild type and mutants were taken for spectral binding studies, and there was no enzyme denaturation during titration. The decreases of the ΔA_{max}, thus, may reflect (1) a decrease of the amount of the substrate that reached the enzyme active site, (2) a decrease of the amount of the substrate in the enzyme active site in an orientation that causes the heme spin shift, or (3) both (1) and (2) occurring simultaneously. Unfortunately, a more definitive interpretation of the data obtained is not possible in the absence of tertiary structures of P450s 27A1 and 11A1.

The Y238A P450 27A1 mutant represents the third group of mutants with normal K_d but increased ΔA_{max}. The increase of ΔA_{max} indicates that more substrate reached the enzyme active site than in the wild-type P450 and that more enzyme−substrate complex was formed.

Finally, the F202K P450 11A1 mutant forms the fourth group characterized by the decreased K_d and ΔA_{max}. About an 8-fold decrease of the apparent K_d and a 6-fold decrease of the ΔA_{max} of this mutant may be interpreted as alteration of cholesterol side-chain orientation in the active site of the mutant. 22*R*-Hydroxycholesterol, for example, binds much more tightly to P450 11A1 than does cholesterol, but it induces a smaller spectral response (*34*) because the side chain adopts a different binding orientation (*35*).

To summarize, neither of the P450 27A1 and P450 11A1 mutants showed a significantly increased K_d that would suggest the direct involvement of the mutated residues in the interaction with substrate. The unchanged K_d also indicates that the mutations did not induce major conformational changes within the enzyme active site. On the other hand, some of the mutations affected substrate orientation in the enzyme active site, as judged by the change in the product pattern. Thus, in the case of two mitochondrial P450s, residues located outside the active site appear to control the orientation of substrate inside the active site.

Uncoupling To Produce Hydrogen Peroxide. In hydroxylation reactions catalyzed by mitochondrial P450s, electrons are transferred from NADPH to P450 by an electron-transport chain that includes a flavoprotein (ferredoxin reductase) and an iron−sulfur protein (ferredoxin). This electron-transfer process is "coupled" when all electrons from NADPH are utilized in substrate hydroxylation reactions and "uncoupled" when a portion of the electrons are transferred to the other acceptors such as O_2. Uncoupling can occur within the electron-transfer chain as well as in the P450 reaction cycle at three different branch points and results in formation of superoxide anion (which spontaneously dismutates to hydrogen peroxide), hydrogen peroxide, and water (*36*). We determined whether hydrogen peroxide is formed in hydroxylation reactions catalyzed by wild-type and mutant forms of P450s 27A1 and 11A1. As shown in Table 3, 58 and 85 nmol of hydrogen peroxide were formed by wild-type P450s 27A1 and 11A1, respectively, under the experimental conditions used. Similar amounts of hydrogen peroxide were produced in the reconstituted systems in the absence of P450 (Table 3), indicating that there is an

Table 3: Hydrogen Peroxide and Product Formation in the P450s 27A1- and 11A1-Dependent Enzymatic Assays

form	H_2O_2, nmol[a]	total products, nmol[a]	H_2O_2/ products
wild-type P450 27A1	58.3 ± 2.7	19.8 ± 1.5	2.9
no P450[b]	53.0 ± 2.7	0	
F207K	69.9 ± 4.2★	4.3 ± 0.4★	16.3
I211K	64.2 ± 2.1	3.9 ± 0.6★	16.5
F215K	87.9 ± 2.7★	3.8 ± 0.4★	23.1
F215A	81.5 ± 4.8★	15.1 ± 1.4★	5.4
F207A/I211A/F215A	81.3 ± 4.8★	6.0 ± 1.2★	13.6
W235A	74.4 ± 1.6★	18.3 ± 3.1	4.1
Y238A	67.3 ± 1.6	14.7 ± 0.7★	4.6
wild-type P450 11A1	84.7 ± 4.1	31.3 ± 0.2	2.7
no P450[c]	77.8 ± 3.5	0	
F202A	125.5 ± 5.8★	2.2 ± 0.5★	57.1
F202K	165.5 ± 1.1★	17.6 ± 1.0★	9.4

[a] The results are the mean ± standard deviation of three to four experiments. Mean values that are significantly different ($p < 0.05$) from those of wild-type P450s 27A1 and 11A1 are designated by a star. [b] No P450 was present in the reconstituted system containing 1 mM NADPH, 1 μM Adr, 4 μM Adr, and 50 μM 5β-cholestane-3α,7α,12α-triol. [c] No P450 was present in the reconstituted system containing 1 mM NADPH, 2 μM Adr, 10 μM Adr, and 50 μM cholesterol.

uncoupling of electron transport in the NADPH → adrenodoxin reductase → adrenodoxin chain (the names of ferredoxin reductase and ferredoxin, respectively, that we used in the assay), resulting in H_2O_2 accumulation. These data agree with those in a previously published report describing electron leakage from the electron-transfer chain, including NADPH−adrenodoxin reductase−adrenodoxin−P450 11A1 (*37*). Under identical conditions, mutant P450s produced more hydrogen peroxide per nanomole of total products than did the corresponding wild-type P450s (Table 3). In P450 27A-dependent assays, the H_2O_2/product ratio was the highest in reactions catalyzed by the F215K mutant, followed by the F207K, I211K, F207A/I211A/F215A, F215A, Y238A, and W235A mutants (Table 3). In P450 11A1-dependent assays, this ratio was much higher for the F202A mutant than for the F202K mutant.

Elution profiles of mutant P450s from an adrenodoxin−Sepharose column (not shown) were unchanged, indicating that interaction with adrenodoxin was not significantly affected by the mutations. We speculate that electron transfer between adrenodoxin and mutant P450s was not affected, and elevated formation of hydrogen peroxide in reactions catalyzed by mutant P450s is due to the uncoupling within the P450 catalytic cycle. The results thus indicate that P450 27A1 and P450 11A1 mutations increased the amounts of the substrate in the P450 active site in unfavorable orientations relative to the activated oxygen, and these unfavorable orientations compromised substrate hydroxylations.

DISCUSSION

By alignment of P450s 27A1 and 11A1 with P450s of known structure, we were able to locate the amino acid sequences of the putative helices F and G and the F−G loop (Figure 1). It is the region of the P450 structure which was shown to be important for substrate access/interaction in structurally characterized P450s 101, 107A1, 2C5, and 102 (*8*, *11*, *13*, *38*). The precise structure of F and G helices and of the F−G loop in P450s 27A1 and 11A1 is, of course, unknown. However, the putative helices and loop (Figure 1) are certainly good estimates, and all of the residues examined in this study must lie within this region.

Unchanged dissociation constants of the Phe-207, Ile-211, Phe-215, Trp-235, and Tyr-238 P450 27A1 mutants clearly rule out the direct interaction of these residues with 5β-cholestane-3α,7α,12α-triol and indicate that the mutations did not cause significant structural perturbations within the enzyme active site. Similar properties of the F207K, I211K, and F215K mutants also suggest that Phe-207, Ile-211, and Phe-215 are located outside of the P450 27A1 active site. Only the C-terminal part of helix F forms the ceiling of the substrate-binding pocket in P450s 102, 107A1, 101, and 2C5. If Phe-215 is indeed in the P450 27A1 active site, replacement of Phe-207 and Ile-211, which are supposedly located outside of the active site, should lead to changes (if any) that are different from those caused by the F215K mutation. However, as with the F215K mutant, the F207K and I211K mutants exhibited significantly decreased enzymatic activity and elevated hydrogen peroxide formation, whereas the apparent binding constant for the substrate was not altered.

Our site-directed mutagenesis data are concordant with notion that the F and G helices form the sides of the substrate-access channel in P450 27A1, as they do in P450 102, and residues lining the substrate-access channel control the delivery of correctly oriented substrate to the enzyme active site. Enhancement of the ability to perform 24- and 25-hydroxylations, acquisition of the capacity to cleave the C−C bond, and reduction of the ΔA_{max} of the I211K and F215K mutants clearly demonstrate that a portion of the substrate in the active site of these P450s is in an altered orientation. We, thus, speculate that Phe-207, Ile-211, Phe-215, and Tyr-238 line the interior of the substrate-access channel. Phe-215 is probably located near the molecule's surface and may even occlude the channel entrance, whereas Ile-211 and Phe-207 are buried deeper inside the channel, closer to the entrance of the active site. Trp-235 is most likely located on the molecule's surface, because the W235A mutation affected the subcellular distribution of P450 27A1. Tyr-238 is probably located inside the channel at a level between the Phe-215 and Ile-211. All of these residues play a structural role, forming a lock-and-key fit for the substrate. By placing spatial constraints they allow the substrate to enter the access channel only in certain orientation(s) assuming regio- and stereoselectivity. Substitutions of Phe-207, Ile-211, Phe-215, Trp-235, and Tyr-238 with alanine did not prevent the substrate from entering the access channel and, consequently, the active site. However, even these substitutions disrupted the finely tuned mechanism of substrate delivery to the enzyme active site and resulted in a partial loss of enzymatic activity, presumably due to uncoupling. Single replacements of Phe-207, Ile-211, and Phe-215 with a positively charged lysine had much more dramatic consequences than did alanine mutations. First of all, lysine mutations made the hydrophobic interior of the substrate-access channel more polar, thus reducing the propensity of the substrate to partition to the active site. Second, because steric hindrance was introduced as a result of mutation, less substrate reached the enzyme active site. Finally, again because of steric hindrance, a portion of the substrate was delivered to the enzyme active site in an altered orientation(s).

The size of the putative F and G helices and the F−G loop is about the same in the different mitochondrial P450s, and this region contains a number of conserved amino acid residues (Figure 1). Mutations of Phe-202 in P450 11A1, which corresponds to Phe-215 in P450 27A1, also resulted in a significantly decreased enzymatic activity, increased hydrogen peroxide formation, and decreased ΔA_{max}, whereas the apparent K_d was either unchanged or decreased by 10-fold. Thus, in two mitochondrial P450s, residues located outside the active site influence the orientation of substrate inside the active site. The only possible interpretation of the results, in our opinion, is that helix F forms a part of the substrate-access channel in mitochondrial P450s.

To conclude, although the significance of our data will become clearer when the structures of P450s 27A1 and 11A1 are known, our present results provide the first specific information pertaining to the substrate-access channel and the additional mechanism that controls regioselectivity of hydroxylation in mitochondrial P450s. The data indicate the presence of the substrate-access channel in this important subset of P450s, identify the putative helices F and G as secondary structural elements that form the sides of the channel, and establish the role of conserved phenylalanine (Phe-215 in P450 27A1 and Phe-202 in P450 11A1) as important for delivery of correctly oriented substrate to the active site of mitochondrilal P450s. This study represents a part of ongoing experiments which are being carried out in this laboratory simultaneously with crystallization of P450s 27A1 and 11A1.

ACKNOWLEDGMENT

We thank Carolyn Cao for technical assistance. Oligonucleotide synthesis and DNA sequencing were carried out by the Recombinant DNA Laboratory of the NIEHS Center at the University of Texas Medical Branch.

REFERENCES

1. Anderson, K. E., Kok, E., and Javitt, N. B. (1972) *J. Clin. Invest. 51*, 112−117.
2. Björkhem, I. (1992) *J. Lipid Res. 33*, 455−471.
3. Waterman, M. R., and Simpson, E. R. (1985) *Mol. Cell. Endocrinol. 39*, 81−89.
4. Cali, J. J., and Russell, D. W. (1991) *J. Biol. Chem. 266*, 7774−7778.
5. Morohashi, K., Fujii-Kuriyama, Y., Okada, Y., Sogawa, K., Hirose, T., Inayama, S., and Omura, T. (1984) *Proc. Natl. Acad. Sci U.S.A. 81*, 4647−4651.
6. Wada, A., and Waterman, M. R. (1992) *J. Biol. Chem. 267*, 22877−22882.
7. Pikuleva, I. A., Björkhem, I., and Waterman, M. R. (1997) *Arch. Biochem. Biophys. 343*, 123−130.
8. Poulos, T. L., Finzel, B. C., and Howard, A. J. (1987) *J. Mol. Biol. 195*, 687−700.
9. Ravichandran, K. G., Boddupalli, S. S., Hasemann, C. A., Peterson, J. A., and Deisenhofer, J. (1993) *Science 261*, 731−736.
10. Hasemann, C. A., Ravichandran, K. G., Peterson, J. A., and Deisenhofer, J. (1994) *J. Mol. Biol. 236*, 1169−1185.
11. Cupp-Vickery, J. R., and Poulos, T. L. (1995) *Nat. Struct. Biol. 2*, 144−153.
12. Park, S. Y., Shimizy, H., Adachi, S., Nakagawa, A., Tanaka, I., Nakahara, K., Shoun, H., Obayashi, E., Nakamura, H., Iizuka, T., and Shiro, Y. (1997) *Nat. Struct. Biol. 4*, 827−832.
13. Williams, P. A., Cosme, J., Sridhar, V., Johnson, E. F., and McRee, D. E. (2000) *Mol. Cell 5*, 121−131.
14. Yano, J. K., Koo, L. S., Schuller, D. J., Li, H., Ortiz de Montellano, P., and Poulos, T. (2000) *J. Biol. Chem. 275*, 31086−31092.
15. Graham, S., and Peterson, J. A. (1999) *Arch. Biochem. Biophys. 369*, 24−29.
16. Wachenfeldt, C., and Johnson, E. F. (1995) in *Cytochrome P450*: *Structure, Mechanism, and Biochemistry* (Ortiz de Montellano, P. R., Ed.) 2nd ed., pp 183−244, Plenum Publishing Corp., New York.
17. Graham-Lorence, S., Amarneh, B., White, R. E., Peterson, J. A., and Simpson, E. R. (1995) *Protein Sci. 4*, 1065−1080.
18. Pikuleva, I. A., Mackman, L. R., Kagawa, N., Waterman, M. R., and Ortiz de Montellano, P. R. (1995) *Arch. Biochem. Biophys. 322*, 189−197.
19. Pikuleva, I. A., Babiker, A., Waterman, M. R., and Björkhem, I. (1998) *J. Biol. Chem. 273*, 18153−18160.
20. Pikuleva, I. A., Cao, C., and Waterman, M. R. (1999) *J. Biol. Chem. 274*, 2045−2052.
21. Pitha, J., Irie, T., Sklar, P. B., and Nye, J. S. (1988) *Life Sci. 43*, 493−502.
22. Omura, T., and Sato, R. (1964) *J. Biol. Chem. 239*, 2370−2378.
23. Jiang, Z.-Y., Woollard, A. C. S., and Wolff, S. P. (1990) *FEBS Lett. 268*, 69−71.
24. Fang, X., Kobayashi, Y., and Halpert, J. R. (1997) *FEBS Lett. 416*, 77−80.
25. Pikuleva, I. A., Björkhem, I., and Waterman, M. R. (1996) *Arch. Biochem. Biophys. 334*, 183−192.
26. Cosme, J., and Johnson, E. F. (2000) *J. Biol. Chem. 275*, 2545−2553.
27. Holmberg-Betsholtz, I., Lund, E., Björkhem, I., and Wikvall, K. (1993) *J. Biol. Chem. 268*, 11079−11085.
28. Lund, E., Björkhem, I., Furster, C., and Wikvall, K. (1993) *Biochim. Biophys. Acta 1166*, 177−182.
29. Kihara, K., Noma, Y., Tsuda, K., Watanabe, T., Yamamoto, Y., Une, M., and Hoshita, T. (1986) *J. Lipid Res. 27*, 393−397.
30. Kuroki, S., Shimazu, K., Kuwabara, M., Une, M., Kihara, K., Kuramoto, T., and Hoshita, T. (1985) *J. Lipid Res. 26*, 230−240.
31. Cronholm, T., and Johanson, G. (1970) *Eur. J. Biochem. 16*, 373−381.
32. Lambeth, J. D., Kitchen, S. E., Farooqui, A. A., Tuckey, R., and Kamin, H. (1982) *J. Biol. Chem. 257*, 1876−1884.
33. Eneroth, P., and Gustafsson, J.-Å. (1969) *FEBS Lett. 5*, 99−103.
34. Heyl, B. L., Tyrrell, D. J., and Lambeth, J. D. (1986) *J. Biol. Chem. 261*, 2743−2749.
35. Lambeth, D. (1986) *Endocr. Res. 12*, 371−392.
36. Mueller, E. J., Loida, P. J., and Sligar, S. G. (1995) in *Cytochrome P450: Structure, Mechanism, and Biochemistry* (Ortiz de Montellano, P. R., Ed.) 2nd ed., pp 83−124, Plenum Publishing Corp., New York.
37. Hanukoglu, I., Rapoport, R., Weiner, L., and Sklan, D. (1993) *Arch. Biochem. Biophys. 305*, 489−498.
38. Li, H., and Poulos, T. L. (1997) *Nat. Struct. Biol. 4*, 140−146.
39. Nelson, D. R., Koymans, L., Kamataki, T., Stegeman, J. J., Feyereisen, R., Waxman, D. J., Waterman, M. R., Gotoh, O., Coon, M. J., Estabrook, R. W., Gunsalus, I. C., and Nebert, D. W. (1996) *Pharmacogenetics 6*, 1−42.

BI010193I